7th European Conference on Structural Dynamics
EURODYN 2008
7-9 July 2008 Southampton

COMPARISON OF PARAMETRIC EXCITATION AND EXCITATION OF AN ELASTIC STAY CABLE

V. Denoël[1] and H. Degée[2*]
[1]FNRS, National Fund for Scientific Research, Postdoctoral Researcher
Department of Architecture, Geology, Environment and Constructions
University of Liège, Chemin des Chevreuils, 1, Bât B 52/3, 4000 Liège
E-mail: V.Denoel@ulg.ac.be

[2]FNRS, National Fund for Scientific Research, Research Associate
Department of Architecture, Geology, Environment and Constructions
University of Liège, Chemin des Chevreuils, 1, Bât B 52/3, 4000 Liège
E-mail: H.Degee@ulg.ac.be

Keywords: parametric excitation, cable excitation, stay cable, bridge

ABSTRACT

In cable-stayed bridge applications, the vertical vibrations of a bridge deck induce vertical motions of the cable anchors that may cause large amplitudes oscillations of the cables. This vertical motion is not collinear with the cable chord and can be split into a transverse and an axial component. The latter one is responsible for a parametric excitation. Since this phenomenon leads to serious dynamic instability, whereas the transverse component provides simple resonances only, the transverse anchor motion is often disregarded or considered in a separate analysis. However, because of the cable's non linear behaviour, the response of the cable under both components cannot simply be added. It is thus important to consider at once this actual "cable excitation", rather than approaching it by an axial excitation, as often reported in the study of parametric excitations. In this paper, the difference between the two modes of excitation is illustrated with a finite element model. The simplicity of the model allows an efficient parametric study of the vibrations of a cable under both excitations, for various cable inclinations and anchor frequencies.

1 INTRODUCTION

The cable-stayed bearing system has been widely used in civil engineering applications since the 1950's ([1]). Because the stay cables offer to the bridge deck close vertical supports, the bending moments along the deck are rather small. Today's cable-stayed bridge decks are therefore very thin (~1/100th of the span). This results in reasonably light structures however

susceptible to be dynamically excited. The vertical vibrations of a bridge deck are mainly induced by the wind and the traffic. As they result in vertical movements of the cable anchors, they may induce large amplitude cable vibrations ([2], [3]).

In typical applications, the inclination of stay cables runs from 20° to 45° with respect to the horizontal (Fig. 1). For a typical stay cable, a vertical anchor movement is not collinear with the cable chord; this kind of excitation is somehow intermediate between the seismic excitation (transverse movement) and the axial excitation (as considered in the study of parametric excitations).

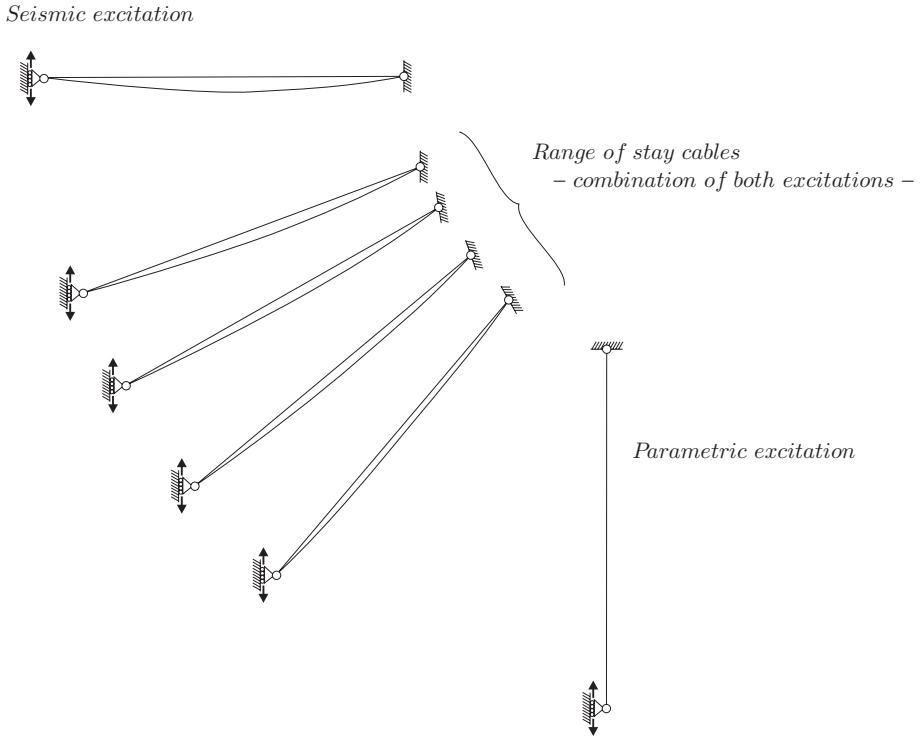

Figure 1. The anchor movements of stay cables are not collinear with the cable chord.

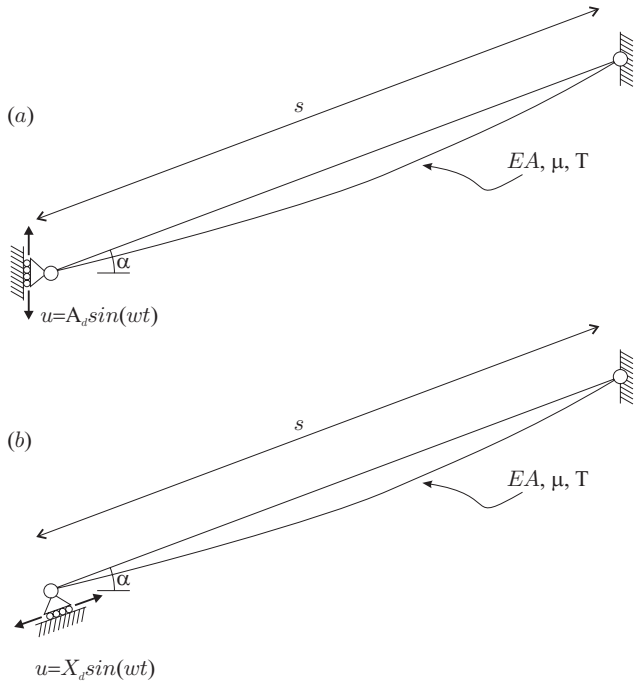

Figure 2. Difference between the stay cable excitation (a) and the parametric excitation (b).

Because of the non linear behaviour of the cable, the effects of both components cannot be solved independently and superimposed. Since it is known that the parametric excitation induces larger amplitudes, the transverse component of the anchor movement is often disregarded (Fig. 2). The stay cable excitation is therefore replaced by a parametric excitation.

In order to illustrate the differences between them, the computation of the cable response is performed for both anchor movement. Parameters of the model have to include the cable stiffness *EA*, the mass per unit length μ and the damping ratio ξ. The length of the cable at rest *L* is smaller than the distance *s* between the anchors, resulting in a static tension *T(s)* in the cable. The movement of the support is supposed to be a harmonic motion with amplitude A_d or X_d and circular frequency ω_d.

A brief overview of the phenomenology of parametric excitation is given in section 2; then the numerical model considered for the study of cable vibrations is presented and benchmarked (section 3) and finally both kinds of excitation are compared (section 4).

2 PHENOMENOLGY

Figure 3 depicts illustrative sketches of seismic and axial excitations. The arrows symbolize the velocity of the cable. The time histories represent the mid-span displacement of a cable, characterized by the quantities given in Table 1, and computed with the numerical model described in section 4.

In the case of seismic excitation (subfigures a, b), waves are initiated at the moving end. Each elementary wave moves across the cable, reflects itself at the other end and continuously adds up to the other waves. Because of structural damping, however very low for stay cables, the amplitude of each elementary wave decreases until it definitely disappears. When the frequency of the anchor movement is equal to the fundamental frequency of the cable, the simple resonance phenomenon takes place. As soon as the cable response reaches a significant amplitude, the stiffness of the cable depends on its amplitude. This stiffness is often supposed to be a cubic function of the displacement ([4]) but is actually more rigorously described by Bleich's formula ([5]). This explains the beating phenomenon observed in Fig. 3-a. When the frequency of the anchor movement is tuned to twice the fundamental frequency of the cable (i.e. to the second natural frequency for a taut-strip, [6]), another simple resonance phenomenon takes place in the second mode. In this case, it can be observed that the displacement at mid-span is very small and the displacement at fourth-span exhibits again a beating shape (Fig. 3-b).

The parametric excitation (subfigures c, d), is due to the oscillations of axial force in the cable, resulting essentially from an axial anchor movement. Such an excitation is likely to introduce forces into the system, when the cable is taught and the anchors are getting away from each other. The circles in the left-hand sketches indicate when these conditions are met. This occurs once per fundamental cable period if the frequency of the anchor movement corresponds to the fundamental frequency (Fig. 3-c), and twice for a doubled excitation frequency (Fig. 3-d).

L	250 m
s	251 m
ξ	0.1%
μ	176.6 kg/m
EA	$4.725.10^9$ N

Table 1: Characteristics of the cable considered for the illustration of Fig. 3.
α=0° for (a), (b); α=89° for (c), (d).

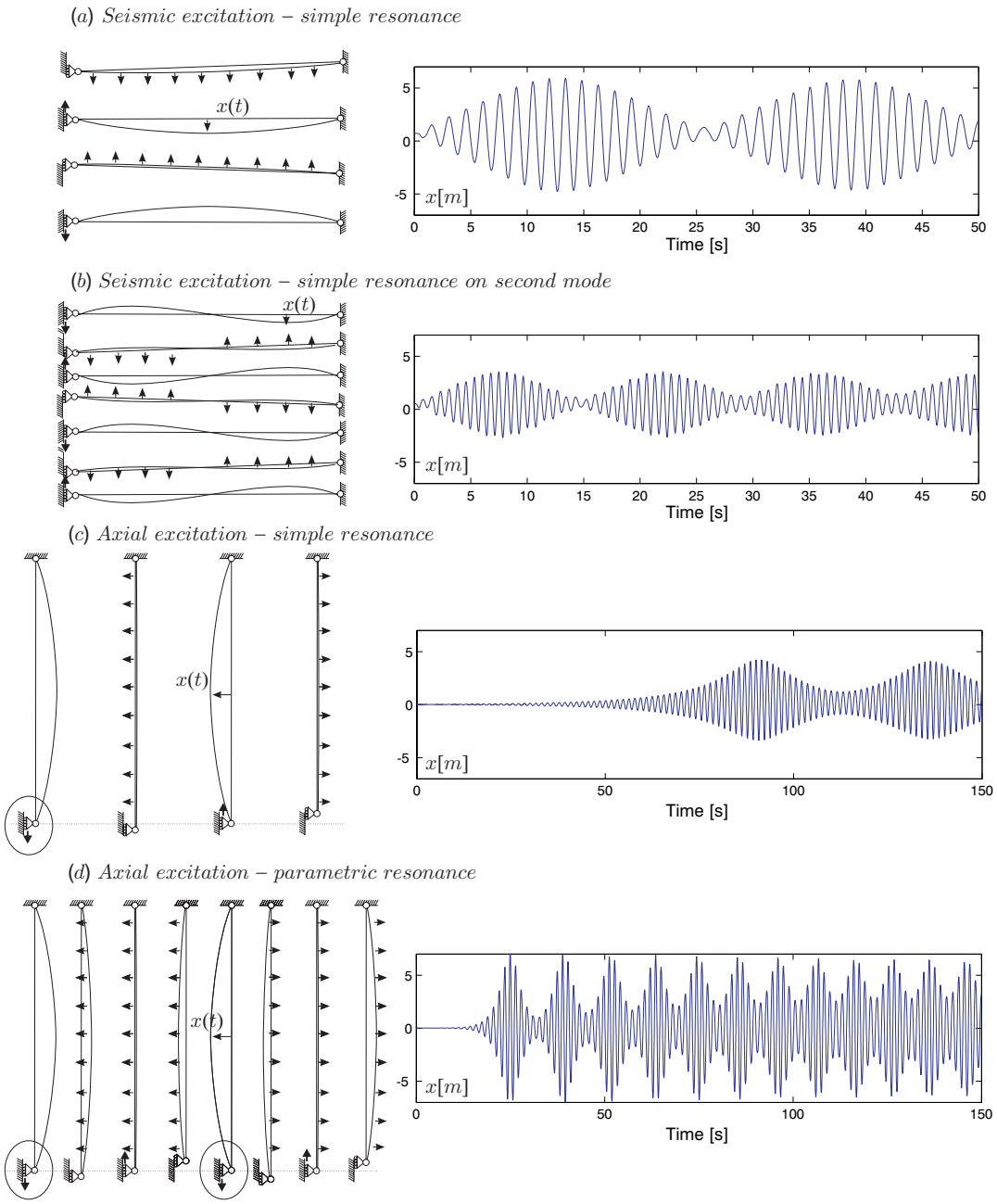

Figure 3. Illustration of seismic and axial excitations. The frequency of the anchor movement is equal to the fundamental cable frequency (a) and (c), or to twice its value (b) and (d).

The oscillations of a cable under axial excitation are described by means of a Mathieu differential equation. The stability of this equation has been widely studied in the literature (e.g. [7]; [8]). In the range of cable tautness generally encountered in cable-stayed bridge applications, it can be demonstrated that a dynamic instability in the first mode (the *k=1* parametric excitation) occurs when:

- the excitation frequency is close to $2\omega_0/k$ ($k=1,2,\ldots$), where ω_0 is the fundamental circular frequency, and
- the amplitude of the anchor motion is larger than a certain threshold function of the structural damping.

It has to be noticed that the larger k is, the higher the excitation amplitude threshold is (Fig. 4). The *k=1* parametric excitation is likely to produce the largest cable amplitudes in the

first mode. As the cable tautness is large, the second natural frequency is often close to the twice the first one, leading to a confusion between the *k=1* parametric excitation in the first mode and the simple resonance in the second mode (which presents however a strictly different shape).

Likewise, the *k=2* parametric excitation occurs when the excitation frequency equals the first natural frequency, leading to a confusion between simple resonance and *k=2* parametric resonance in the first mode.

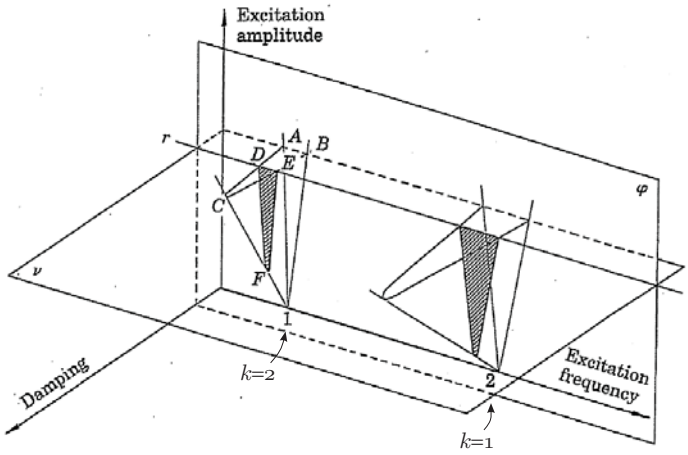

Figure 4. Illustration of the instability zones of the Mathieu equation (from [9]).

3 NUMERICAL MODEL

The dynamic behaviour of the cable is studied with the finite element method. Because of the non linearity of the cable's behaviour, large displacement finite elements have to be considered. In order to keep a simple mathematical formulation, a 2-node truss element expressed in a corotational updated reference system is used ([10]).

The initial configuration is a straight line with length *L*; the discretisation is obtained by dividing it into *n* finite elements. The initial element lengths and the locations of the nodes in the stress-free configuration are denoted by l_i and (x_i,y_i), $i=1,\ldots n+1$ (Fig. 5). The unknown displacements of the nodes are collected in a $(2(n+1)\times 1)$ vector $\boldsymbol{u}$ with *u(1)* and *u(2)* corresponding respectively to the horizontal (x) and vertical (y) displacements at the lower end, and *u(2n+1)* and *u(2n+2)* to the displacements at the top.

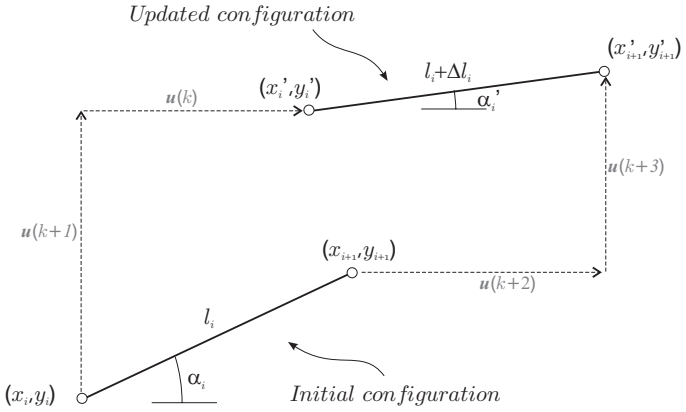

Figure 5. Initial and updated configurations (finite element model).

The location of an element's nodes in the updated configuration is obtained by adding the relevant components of $\boldsymbol{u}$ to the coordinates in the initial configuration. The elongation of this element Δl_i and its updated inclination α_i' are straightforwardly deduced from the updated coordinates by simple geometrical relations:

$$\begin{aligned} \Delta l_i(\boldsymbol{u}) &= \sqrt{\left(x'_{i+1} - x'_i\right)^2 + \left(y'_{i+1} - y'_i\right)^2} - l_i \\ \alpha_i'(\boldsymbol{u}) &= \arctan \frac{y'_{i+1} - y'_i}{l_i + \Delta l_i} \end{aligned} \tag{1}$$

These finite rotation and elongation are the non linear essence of the finite element formulation. The elementary internal forces result from the element elongation only (truss element). As a function of the unknown displacement field **u**, they are expressed in the global coordinates by:

$$\boldsymbol{f}_i^G(\boldsymbol{u}) = \begin{bmatrix} -\cos\alpha_i' \\ -\sin\alpha_i' \\ \cos\alpha_i' \\ \sin\alpha_i' \end{bmatrix} \frac{EA\Delta l_i(\boldsymbol{u})}{l_i} \tag{2}$$

where *EA* is the axial stiffness of the cable.

The resultant of the internal forces $\boldsymbol{f}^G$ is a (*2(n+1)×1*) vector obtained by the assembly of elementary internal forces. This is formally written by means of localisation matrices $\boldsymbol{L_i}$. In static equilibrium, the internal forces balance the externally applied forces $\boldsymbol{p}$ and the reaction forces $\boldsymbol{r}$:

$$\boldsymbol{f}^G(\boldsymbol{u}) = \sum_{i=1}^{n} \boldsymbol{L}_i \boldsymbol{f}_i^G(\boldsymbol{u}) = \boldsymbol{p} + \boldsymbol{r} \tag{3}$$

The boundary conditions are given by:

$$\begin{aligned} \boldsymbol{u}(1) &= 0 \quad ; \qquad \boldsymbol{u}(2n+1) = (s - L)\cos\alpha \\ \boldsymbol{u}(2) &= 0 \quad ; \qquad \boldsymbol{u}(2n+2) = (s - L)\sin\alpha \end{aligned} \tag{4}$$

where *L* is the length of the cable at rest, *s* is the distance between the supports and α is the chord inclination.

The pre-tension in the cable is accounted for by imposing the displacement at the top. In Eq. (3), the equations involving a non-zero reaction are simply removed, leading thus to a set of *2n-2* equations with *2n-2* unknowns. The set of equations is solved with the non linear solver function of MatLab (fsolve). If $\boldsymbol{p}$ contains the forces energetically equivalent to the self-weight, the solution of Eqs. (3) and (4) supplies the deflections $\boldsymbol{u_{stat}}$ of the cable under both self-weight and pre-tension. This deformation state is used as an initial condition for the subsequent dynamic analysis.

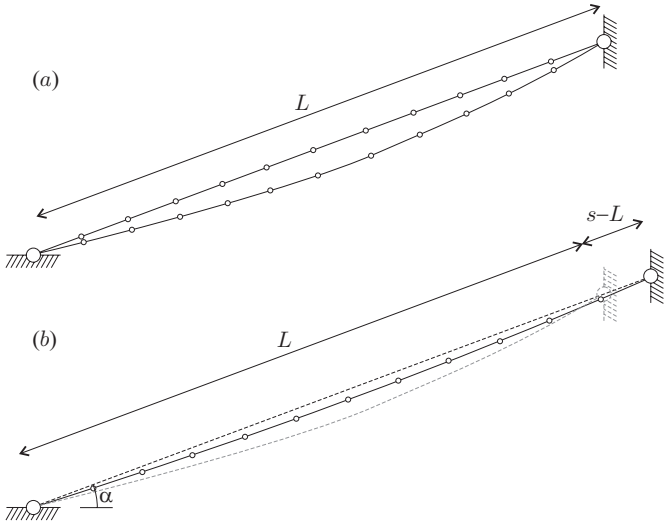

Figure 6. (a) Cable under self weight – (b) Cable under self weight and tension. (*L* is the length of the cable at rest, *s* is the distance between the anchors and α is the chord inclination)

The elements of the tangent stiffness matrix corresponding to an equilibrium state $\boldsymbol{u}$ is obtained by:

$$\boldsymbol{K}_{ij}\left(\boldsymbol{u}\right)=\frac{\partial \boldsymbol{f}_j^{\,G}}{\partial \boldsymbol{u}_i} \tag{5}$$

In a dynamic analysis, the inertial forces applied on the elements have to be summed up. They are expressed by means of a lumped mass matrix $\boldsymbol{M}$. From the knowledge of the initial tangent stiffness matrix corresponding to the static equilibrium $\boldsymbol{K}(\boldsymbol{u}_{stat})$, a damping matrix $\boldsymbol{C}$ is formed in accordance to the Rayleigh damping ([11]), by imposing a damping coefficient $\xi=0.1\%$ in the first two modes. This matrix is kept constant during the dynamic analysis. The equations of motion are then expressed by the following non linear set of differential equations:

$$\boldsymbol{M}\ddot{\boldsymbol{u}}+\boldsymbol{C}\dot{\boldsymbol{u}}+\boldsymbol{f}^{\boldsymbol{G}}\left(\boldsymbol{u}\right)=\boldsymbol{p}+\boldsymbol{r} \tag{6}$$

Since the lumped mass matrix is not singular this problem can be written in a state space, and then transformed to a first order set of ODE's.

The anchor motion is imposed as in Eq. (4):

$$\boldsymbol{u}(1)=X_d\cos\phi \quad ; \qquad \boldsymbol{u}(2)=X_d\sin\phi \tag{7}$$

where ϕ is the inclination of the anchor motion with respect to the horizontal and X is the amplitude of the motion. The equations related to the fixed degrees of freedom are disregarded, and the *ode45* solver implemented in MatLab is used for the solution.

4 RESULTS

4.1 Validation of the model

The numerical procedure described in section 3 is used to investigate the difference between the dynamic response of a cable under parametric and cable excitations.

In order to validate the numerical model, a horizontal cable represented by 8 large displacement finite elements is considered (Fig. 7). The basic characteristics of this cable are given in Table 2, together with some resulting information as the fundamental circular frequency, the pre-tension in the stay cable and the Irvine parameter (as defined in [4]). These basic characteristics correspond to a stay cable of the Ben-Ahin bridge (Belgium) investigated in [9]. Figure 7 represents the displacements at mid-span under a 5 cm anchor movement, and two different excitation frequencies ($\omega_d=\omega_0=7.26rad/s$ and $\omega_d=2.02\omega_0=15.39rad/s$). The match between these results and those presented in [9], obtained with 12 more sophisticated isoparametric cable elements, demonstrates the accuracy of the considered approach, in spite of its simplicity.

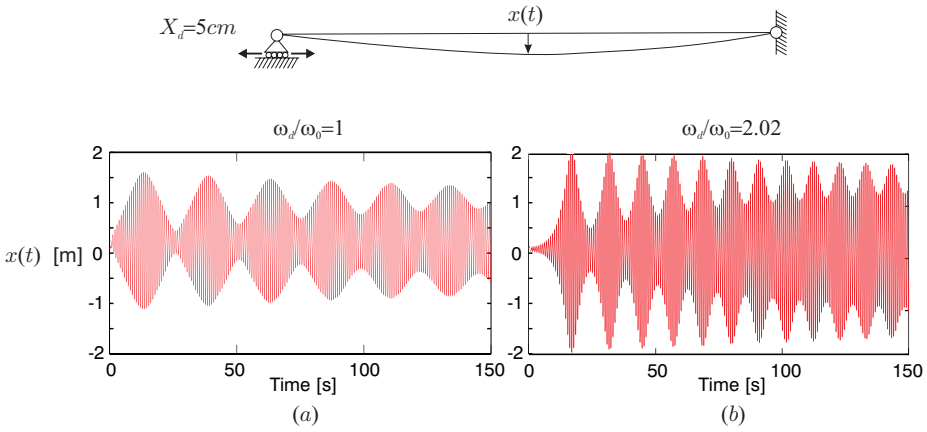

Figure 7. Time histories of the mid-span displacement of a horizontal cable under axial loading α=0°, ϕ=0° – Simple resonance (a) and Parametric resonance (b)

Basic data		Resulting quantities	
L	110.5 m	α=0°	ω_0=7.261 rad/s
s	110.812 m		T=4.89 MN
α	0°, 45°, 89°		λ^2=0.073
ξ	0.1%	α=45°	ω_0=7.609 rad/s
μ	64.76 kg/m		T=4.86 MN
EA	1732.5 MN		λ^2=0.073
		α=89°	ω_0=7.590 rad/s
			T=4.85 MN
			$\lambda^2=1.9.10^{-5}$

Table 2: Characteristics of the cable considered for the validation of the numerical model (Fig. 7) and for the parametric study (Fig. 8).

4.2 Study of parametric excitations and excitation of an elastic stay cable

Because of the efficiency of the considered numerical model, a parametric study of the cable under different anchor movements and different cable inclinations can be performed in detail. Two anchor movement directions are considered:

- axial (Fig. 8-a, b, c), in order to simulate the parametric excitation,
- vertical (Fig. 8-d, e, f) in order to simulate the cable excitation.

In each case, three cable inclinations are considered. The inclination of the vertical cable is set at 89° to avoid the necessity to apply an initial perturbation.

Each subfigure of Fig. 8 represents the envelope of the *150-s* transverse displacements of the cable at mid- and fourth-span, under different excitation frequencies. As an example, the results of Fig.7 correspond to two points in Fig. 8-a.

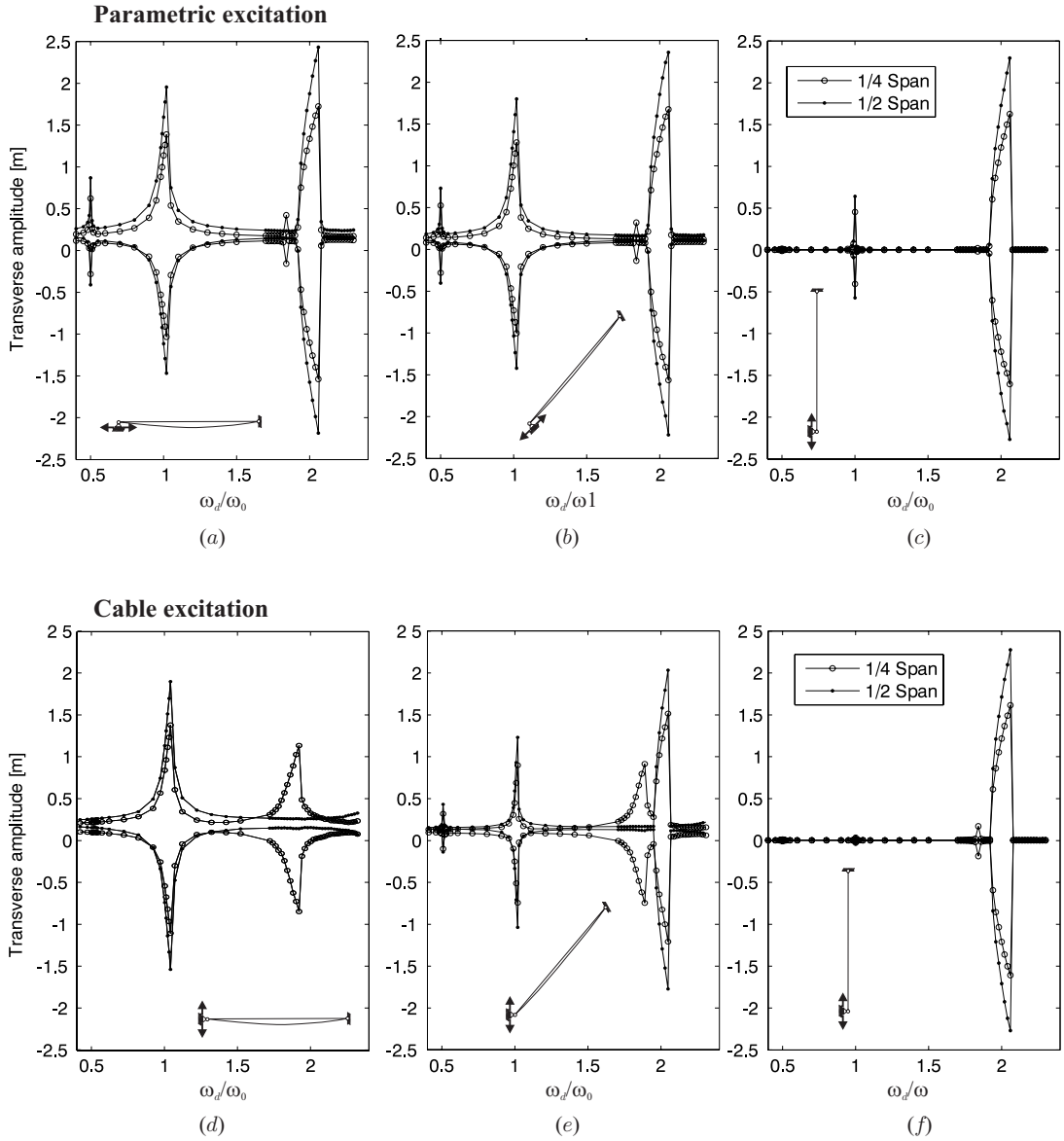

Figure 8. Envelopes of the cable displacement at mid- and fourth- span for different anchor movement frequencies. The anchor motion is axial (a) to (c), or vertical (d) to (f).

The superposition of the extreme displacements at mid- and fourth-span allows the interpretation of the mode into which the structure is deformed. When the ratio between these extremes is close to $\sqrt{2}/2$, the response is mainly in the first mode; when the displacement at mid-span is much smaller than the displacement at fourth-span, the response is mainly in the second mode.

The deformations of an axially excited cable (subs, (a), (b), (c)) are essentially in the first mode. The *k=1* parametric excitation, corresponding to an anchor frequency equal to twice the fundamental cable frequency, is clearly illustrated. Because the cable tautness (see Irvine parameter [4], λ^2 in Table 2) of this cable is very low, the response to the *k=1* parametric excitation is independent of the cable inclination ([9]).

A vertical cable axially excited (Fig. 8-c) exhibits almost no transverse deformation, except in the vicinity of the *k=1* parametric excitation. This indicates that the parametric excitation is an unstable phenomenon, and that the anchor movement is too small to generate significant *k=2* (and higher) instabilities.

This gives also a meaning to the peaks observed around $\omega_d/\omega_0=1$ in Fig. 8-a and 8-b: as the contribution of the *k=2* parametric excitation is very small, they have to be considered mainly as simple resonance peaks.

The seismic excitation is illustrated in Fig. 8-d. As mentioned in section 2, the behaviour of the cable presents simple resonances only. The shape of the second mode is easily identified by means of the displacement at fourth-span. The similarity of the resonance peaks around $\omega_d/\omega_0=1$ in Fig. 8-a and 8-d strengthens the former statement.

The only difference between the results of Figs. 8-c and 8-f is the direction of the anchor movement, which is either axial (i.e. 89° with the horizontal) or vertical, respectively.

The results of the most relevant configuration are obviously those presented in Fig. 8-e. This cable has an intermediate behaviour between the previously commented situations. The simple resonance peak corresponding to the first mode is narrower. The simple resonance peak corresponding to the second mode exists (because of the transverse component of the anchor movement) but merges with the adjacent parametric resonance peak.

In a real application, the anchor movement results from wind and traffic loadings. At the considered time scale, this loading cannot be considered as stationary. Consequently, the anchor movement can be seen as having a variable frequency during the establishment of the steady-state. If it is considered that the actual peaks of the frequency response are narrower than what is predicted with an axial excitation (as shown in Fig. 8), it is much more difficult for the excitation to lock onto the resonance frequencies. This may explain why the large amplitude vibrations usually predicted are seldom observed in built-in bridges. Another convincing argument is the actual proximity of two peaks corresponding to different mode shapes. Because of the variability of the loading frequency, the cable may have to jump, from peak-to peak, i.e. from time to time between two different modes. This induces evidently transient phases, resulting thus in a longer duration for the stationary states to settle.

5 CONCLUSIONS

The dynamics of a cable undergoing an anchor movement are modelled with a simple finite element approach, based on large displacement truss elements expressed in a corotational reference system. This fast but accurate model allows studying efficiently the response of the cable under various excitation frequencies, excitation directions and cable inclinations.

The frequency response function of a usual stay cable subjected to a realistic vertical anchor movement exhibits a particular shape. Its approximation by an axial anchor

movement, as usually performed when studying the effects of the parametric excitation, leads to significantly different results. The realistic anchor movement provides a narrower resonance peak and two merging peaks corresponding to different modes shapes. This clarifies the reasons why large amplitude oscillations of stay cable are numerically predicted but seldom observed in real bridges.

ACKNOWLEDGMENTS

The authors would like to acknowledge the Belgian Fund for Scientific Research.

REFERENCES

[1] N. J. Gimsing, The modern cable-stayed bridge – 50 years of development from 1955 to 2005, *Innovation of Structures*, 1, 47-64, 2005.

[2] A. J. Persoon, The wind induced response of a cable stayed bridge, *ICE Bridge Aerodynamics*, 73-77, 1981.

[3] Q. X. Wu, K. Takahashi, B. Chen, Using cable finite elements to analyse parametric vibrations of stay cables in cable-stayed bridges, *Structural Engineering Mechanics*, 23, 691-711, 2006.

[4] M. Irvine, *Cable Structures*, Dover Publications, 1992.

[5] F. Bleich, *The mathematical theory of vibration in suspension bridge.* Washington, D.C.: US. Government Printing Offices, 1950.

[6] H. M. Irvine, T. K. Caughey, The linear theory of free vibrations of a suspended cable, *Proceedings of the Royal Society of London*, Series A, 314, 299-315, 1974.

[7] G. Tagata, Harmonically forced finite amplitude vibration of a string. *Journal of Sound and Vibration*, 51, 483-492, 1977.

[8] A. Pinto da Costa, J. A. C. Martins, F. Branco, J. L. Lilien, Oscillations of bridge stay cables induced by periodic motion of deck and/or towers. *Journal of Engineering Mechanics*, 122, 613-622, 1996.

[9] J. L. Lilien, A. Pinto da Costa, Vibration amplitudes caused by parametric excitation of cable stayed structures. *Journal of Sound and Vibration*, 174, 69-90, 1994.

[10] O. C. Zienkievic, *The finite element method in engineering*, Pergamon Press, Oxford, 1982.

[11] R. W. Clough, J. Penzien, *Dynamics of Stuctures*, McGraw-Hill College, 1975.